Transient free convection with mass transfer from an isothermal vertical flat plate embedded in a porous medium

Jiin-Yuh Jang and Jong-Ren Ni
Department of Mechanical Engineering, National Cheng-Kung University, Tainan, Taiwan 70101, Republic of China

Received 23 December 1987 and accepted for publication 9 June 1988

The problem of transient free convection in a porous medium adjacent to a vertical semi-infinite flat plate with a simultaneous step change in wall temperature and wall concentration is investigated. Nondimensionalization of the transient boundary-layer equations results in three governing parameters: (1) Le, the Lewis number, (2) N, the buoyancy ratio, and (3) ε, the value of the porosity of the porous medium divided by the ratio of heat capacity of the saturated porous medium to that of the fluid. The resulting nonlinear partial differential equations are solved by an explicit finite-difference method. The numerical results are presented for $0.3 \leq \mathrm{Le} \leq 100$, $0 \leq N \leq 10$, and for $\varepsilon = 0.5$, 1, and 2. It is shown that for a given Le and ε the time required to reach the steady state decreases as N increases; for a given N and ε, when $\mathrm{Le} < 1$, the time decreases as Le increases, while for $\mathrm{Le} \geq 1$, the reverse trend is true; and for a given N and Le, the time increases as ε increases. The final steady-state profiles are in good agreement with similarity solutions. Moreover, a simple relation of predicting the length of time for which a one-dimensional heat/mass transport will exist is obtained.

Keywords: transient flow; natural convection; porous medium; mass transfer

Introduction

There are many free convections in porous media which occur in natural and in technological applications in which flows are simultaneously driven by the differences in temperature and concentration. The applications include the migration of moisture through air contained in fibrous insulations and grain storage installations, and the dispersion of chemical contaminants through water-saturated soil.

Bejan and Khair[1] obtained the similarity solutions for the vertical steady natural convection boundary layer flow in a porous medium resulting from the combined buoyancy mechanism. The steady natural convection phenomenon occurring inside a porous enclosure with both heat and mass transfer from the side was studied by Trevisan and Bejan.[2]

Johnson and Cheng[3] presented the first paper on the transient boundary layer flow over an inclined flat surface in a porous medium without mass transfer. The similarity solutions are obtained for specific variations of wall temperature in both time and position. Ingham, Merkin, and Pop[4] used the asymptotic expansion to investigate the transient free convection flow past a suddenly cooled vertical flat plate surface in a porous medium without mass transfer. Cheng and Pop[5] employed an integral method to analyze the transient free convection boundary layer in a porous medium without mass transfer adjacent to a semi-infinite vertical plate with a step change in wall temperature or surface heat flux. Recently, a related problem of steady and unsteady free convection boundary layer flow past a semi-infinite flat plate, where the wall temperature varies as a power of the distance from the leading edge of the plate, was studied by Ingham and Brown.[6] A numerical solution was also presented that matches the small and large time solutions.

The purpose of this paper is to investigate the transient laminar free convection, involving the simultaneous effects of heat and mass transfer, about a vertical flat plate embedded in a porous medium, with a step change in temperature and concentration. The partial differential equations describing the conservation of mass, momentum, energy, and concentration were solved in their time-dependent form by an explicit finite-difference technique. Representative transient velocity, temperature and concentration profiles, along with the transient average Nusselt and Sherwood numbers, are presented for various values of the governing parameters. As might be expected, the results for a porous medium resemble those for a viscous fluid.[7] However, there are some differences, notably those arising from the boundary conditions and governing equations that differ in the two problems.

Mathematical analysis

The physical model considered in the present paper consists of a semi-infinite vertical flat plate which is embedded in a saturated porous medium. The plate is initially situated in a porous medium saturated with quiescent fluid at uniform temperature T_∞ and concentration C_∞. Then the temperature of the plate is suddenly subjected to a step change from T_∞ to T_w at time $t=0$. Simultaneously the surface concentration is changed from C_∞ to C_w. Consideration is given to this transient, laminar flow with simultaneous heat and mass transfer along the vertical plate.

The following conventional assumptions simplify the analysis. (1) The physical properties are considered to be constant, except for the density term that is associated with the body force. (2) Flow is sufficiently slow so that the convecting fluid and the porous matrix are in local thermodynamic equilibrium. (3) The processes occur at low concentration difference such that the diffusion-thermo and thermodiffusion effects and the interfacial velocity due to mass diffusion can be neglected. (4) Darcy's law and the Boussinesq and boundary layer approximations are employed.

The transient equations that account for the conservation of mass, momentum, energy, and concentration according to the above assumptions are

$$\frac{\partial u}{\partial x}+\frac{\partial v}{\partial y}=0 \tag{1}$$

$$\frac{\partial u}{\partial y}=\frac{\rho_\infty gK}{\mu}\left(\beta_T\frac{\partial T}{\partial y}+\beta_C\frac{\partial C}{\partial y}\right) \tag{2}$$

$$\sigma\frac{\partial T}{\partial t}+u\frac{\partial T}{\partial x}+v\frac{\partial T}{\partial y}=\alpha\frac{\partial^2 T}{\partial y^2} \tag{3}$$

$$\phi\frac{\partial C}{\partial t}+u\frac{\partial C}{\partial x}+v\frac{\partial C}{\partial y}=D\frac{\partial^2 C}{\partial y^2} \tag{4}$$

where the x-coordinate is measured upward along the plate from the leading edge, and the y-coordinate is measured outward normal to the plate; u and v are Darcy's velocity in the x- and y-directions; K is the permeability of the saturated porous media; α and D represent the equivalent thermal and mass diffusivities; β_T and β_C are the coefficients for thermal and concentration expansion; σ is the ratio of heat capacity of the saturated porous medium to that of the fluid; and ϕ denotes the porosity. The other symbols are defined in the Notation.

The associated initial and boundary conditions for Equations 1–4 are simple if we neglect any induced velocity at the surface caused by the mass diffusion effect. They are

$$\begin{aligned}
&t=0: && u=v=0,\quad T=T_\infty,\quad C=C_\infty\\
&x=0: && u=0,\quad T=T_\infty,\quad C=C_\infty\\
&y=0: && v=0,\quad T=T_w,\quad C=C_w\\
&y\to\infty: && u\to 0,\quad T\to T_\infty,\quad C\to C_\infty
\end{aligned} \tag{5}$$

The nondimensional variables are

$$\tau=\frac{t}{\sigma L^2}\mathrm{Ra}_L\alpha,\quad X=\frac{x}{L},\quad Y=\frac{y}{L}\mathrm{Ra}_L^{1/2}$$

$$U=\frac{uL}{\mathrm{Ra}_L\alpha},\qquad V=\frac{vL}{\mathrm{Ra}_L^{1/2}\alpha} \tag{6}$$

$$\theta=\frac{T-T_\infty}{T_w-T_\infty},\qquad \lambda=\frac{C-C_\infty}{C_w-C_\infty}$$

where L is the characteristic length of the plate and $\mathrm{Ra}_L=gKL\beta_T(T_w-T_\infty)/\alpha\nu$ is the modified thermal Rayleigh number. In terms of these variables, Equations 1–4 can be expressed as

$$\frac{\partial U}{\partial X}+\frac{\partial V}{\partial Y}=0 \tag{7}$$

$$U=\theta+N\lambda \tag{8}$$

$$\frac{\partial\theta}{\partial\tau}+U\frac{\partial\theta}{\partial X}+V\frac{\partial\theta}{\partial Y}=\frac{\partial^2\theta}{\partial Y^2} \tag{9}$$

$$\varepsilon\frac{\partial\lambda}{\partial\tau}+U\frac{\partial\lambda}{\partial X}+V\frac{\partial\lambda}{\partial Y}=\frac{1}{\mathrm{Le}}\frac{\partial^2\lambda}{\partial Y^2} \tag{10}$$

where $\mathrm{Le}=\alpha/D$ is the Lewis number, $\varepsilon=\phi/\sigma$, and N is the buoyancy ratio, defined as $N=\beta_C(C_w-C_\infty)/\beta_T(T_w-T_\infty)$. This quantity measures the relative significance of species and thermal diffusion in causing the density variation which drives the flow. Note that N is zero for no species diffusion, infinite for no thermal diffusion, and positive for both effects combining to drive the flow. The corresponding initial and boundary conditions are

$$\begin{aligned}
&\tau=0: && U=V=\theta=\lambda=0\\
&X=0: && U=\theta=\lambda=0\\
&Y=0: && V=0,\quad \theta=\lambda=1\\
&Y\to\infty: && U\to 0,\quad \theta,\quad \lambda\to 0
\end{aligned} \tag{11}$$

In general, the Nusselt and Sherwood numbers are used to describe heat and mass transfer characteristics. In the present analysis, the local Nusselt and Sherwood numbers, varying along the plate, are

$$\mathrm{Nu}_x=\frac{q''}{T_w-T_\infty}\frac{x}{k}=-\left(\frac{\partial\theta}{\partial Y}\right)_{Y=0}\mathrm{Ra}_L^{1/2}X \tag{12}$$

Notation

- C Concentration
- D Mass diffusivity
- g Gravitational acceleration
- J'' Mass flux rate
- k Thermal conductivity
- K Permeability
- L Characteristic length of the flat plate
- Le Lewis number $\equiv\alpha/D$
- N Buoyancy ratio parameter $\equiv\beta_C(C_w-C_\infty)/\beta_T(T_w-T_\infty)$
- Nu_x Local Nusselt number
- $\overline{\mathrm{Nu}}_L$ Average Nusselt number
- q'' Heat flux rate
- Ra_L Thermal Rayleigh number $\equiv Kgl\beta_T(T_w-T_\infty)/\alpha\nu$
- Sh_x Local Sherwood number
- $\overline{\mathrm{Sh}}_L$ Average Sherwood number
- t Time
- T Temperature
- u, v x- and y-velocity components
- U, V Dimensionless x- and y-velocities
- x, y Cartesian coordinate along and normal to the plate
- X, Y Dimensionless Cartesian coordinate along and normal to the plate

Greek symbols

- α Thermal diffusivity of fluid-saturated porous medium
- β_C Volumetric coefficient of expansion with concentration
- β_T Volumetric coefficient of thermal expansion
- μ Viscosity
- ν Kinematic viscosity
- ρ Density
- σ Heat capacity ratio
- τ Dimensionless time
- θ Dimensionless temperature $\equiv(T-T_\infty)/(T_w-T_\infty)$
- λ Dimensionless concentration $\equiv(C-C_\infty)/(C_w-C_\infty)$
- ϕ Porosity
- ε ϕ/σ

Subscripts

- x Local property
- w Wall property
- ∞ Porous reservoir property

$$\mathrm{Sh}_x=\frac{J''}{C_w-C_\infty}\frac{x}{D}=-\left(\frac{\partial\lambda}{\partial Y}\right)_{Y=0}\mathrm{Ra}_L^{1/2}X \tag{13}$$

It is of practical interest to determine the average Nusselt and Sherwood numbers for heat and mass transfer calculations. These two quantities are given by

$$\overline{\mathrm{Nu}}_L=-\mathrm{Ra}_L^{1/2}\int_0^1\left(\frac{\partial\theta}{\partial Y}\right)_{Y=0}\mathrm{d}X \tag{14}$$

$$\overline{\mathrm{Sh}}_L=-\mathrm{Ra}_L^{1/2}\int_0^1\left(\frac{\partial\lambda}{\partial Y}\right)_{Y=0}\mathrm{d}X \tag{15}$$

During the initial period of the transient, before the leading edge effect is felt, the V-velocity and the X-derivative terms of the U-velocity, temperature, and concentration in Equations 7–10 are zero, resulting in one-dimensional heat and mass diffusion flow. Thus, before the leading edge is felt, the governing Equations 7–10 reduce to

$$U=\theta+N\lambda \tag{16}$$

$$\frac{\partial\theta}{\partial\tau}=\frac{\partial^2\theta}{\partial Y^2} \tag{17}$$

$$\varepsilon\frac{\partial\lambda}{\partial\tau}=\frac{1}{\mathrm{Le}}\frac{\partial^2\lambda}{\partial Y^2} \tag{18}$$

Therefore, for very short times, pure heat conduction and pure mass diffusion can completely describe the heat and mass transfer mechanisms. It is easily shown that during the one-dimensional portion of the transient, the following closed-form solutions for Equations 17 and 18, subject to the initial and boundary conditions 11, can be obtained:

$$\theta=\mathrm{erfc}\left[\frac{Y}{2}\left(\frac{1}{\tau}\right)^{1/2}\right] \tag{19}$$

$$\lambda=\mathrm{erfc}\left[\frac{Y}{2}\left(\frac{\varepsilon\mathrm{Le}}{\tau}\right)^{1/2}\right] \tag{20}$$

where erfc is the complementary error function. Substituting Equations 19 and 20 into Equations 14 and 15 lets us express the average Nusselt and Sherwood numbers analytically for the initial transient period as follows:

$$\overline{\mathrm{Nu}}_L/\mathrm{Ra}_L^{1/2}=(1/\pi\tau)^{1/2} \tag{21}$$

$$\overline{\mathrm{Sh}}_L\mathrm{Ra}_L^{1/2}=(\varepsilon\mathrm{Le}/\pi\tau)^{1/2} \tag{22}$$

The question of the time duration of the one-dimensional transient in Newtonian fluid has been extensively studied in Refs. 8–10. In Ref. 8 Goldstein and Briggs suggested that a leading-edge effect, which would locally terminate the pure conduction/diffusion phase on a surface of finite length, propagates up the surface in time t a distance

$$X_{p,\max}=\text{maximum value of}\int_0^t u(t)\,\mathrm{d}t \tag{23}$$

where $X_{p,\max}$ is the maximum value of the integral for a given t. This distance is then employed to estimate the transition time, at which point the one-dimensional pure conduction/diffusion solution will be no longer applicable locally, since the leading-edge effects are felt and true convection then takes place. Since the Darcian fluid is considered in the present problem, the maximum value of the velocity $u(y,t)$ during the initial one-dimensional transient occurs on the surface of the plate, and it can be directly obtained from Equation 16 as follows:

$$U_{p,\max}(Y,\tau)=1+N \tag{24}$$

Substituting Equation 24 into Equation 23 and then integrating, have

$$X_{p,\max}=(1+N)\tau \tag{25}$$

Numerical solution procedure

The system of Equations 7–10, together with their corresponding initial and boundary conditions, Equation 11, is solved by using an explicit finite-difference scheme similar to that used in Refs. 11–13. Second-order derivatives are written in central differences, forward differences are used for first-order derivatives in Y and τ, and backward differences are used for X-derivatives. The flow region adjacent to the surface is divided into an $m\times n$ nonuniform grid in the X- and Y-directions, respectively. The derived finite-difference equations are then solved at each grid point in the flow field by marching forward in time.

Since the explicit procedure is employed, the time step $\Delta\tau$ is restricted due to stability considerations. Using the analysis prescribed in detail by Carnahan *et al.*[14] and Anderson *et al.*,[15] we can easily show that

$$\Delta\tau\leq\min\left\{\left[\frac{U}{\Delta X}+\frac{|V|}{\Delta Y}+\frac{2}{(\Delta Y)^2}\right]^{-1},\left[\frac{1}{\varepsilon}\left[\frac{U}{\Delta X}+\frac{|V|}{\Delta Y}+\frac{1}{\mathrm{Le}}\frac{2}{(\Delta Y)^2}\right]\right]^{-1}\right\} \tag{26}$$

This stability criterion is independent of N.

At any given time, the local Nusselt and Sherwood numbers, Equations 12 and 13, are obtained by five-point approximations for the expansion of the derivatives $(\partial\theta/\partial Y)_{Y=0}$ and $(\partial\lambda/\partial Y)_{Y=0}$. As to the evaluation of the average Nusselt and Sherwood numbers, Equations 14 and 15 are integrated by using the Simpson's rule to obtain values for $\overline{\mathrm{Nu}}_L$ and $\overline{\mathrm{Sh}}_L$.

From a series of preliminary computations with different grid sizes and time steps, the following mesh sizes, with grid of $m=23$ and $n=49$, are adopted:

$$\begin{aligned}&\Delta X=0.02 && (0\leq X\leq 0.2)\\&\Delta X=0.06 && (0.2\leq X\leq 0.6)\\&\Delta X=0.10 && (0.6\leq X\leq 1.0)\\&\Delta Y=0.10 && (0\leq Y\leq 2)\\&\Delta Y=0.40 && (2\leq Y\leq 10)\\&\Delta Y=0.50 && (10\leq Y\leq 14)\end{aligned} \tag{26}$$

The time step $\Delta\tau$ is varied between 0.0005 and 0.001, depending on the chosen mesh sizes, Le numbers, and ε, to ensure the stability and accuracy of the numerical scheme. In order to check convergence of the finite difference solutions, the spatial grid sizes are doubled, accompanied by a change in $\Delta\tau$, and the results for the two solutions are compared. Table 1 presents the average Nusselt/Sherwood numbers in increasing time values for $\varepsilon=1$, $N=2$, and $\mathrm{Le}=1$, calculated with grids of 23×49 and 45×97, and uniform time steps $\Delta\tau$ of 0.001 and 0.0005. It indicates that the differences of the respective average Nusselt/Sherwood numbers among the choices for grid sizes and time steps described in Table 1 are less than 3%. It is also shown that decreasing the time step and increasing the grid number result in a change in the transient local temperature and concentration profiles across the boundary layer of not more than 1%. However, the use of the finer mesh and smaller time step will require much more memory and a sixfold increase in computation time. The value $Y=14$ is considered to represent $Y\rightarrow\infty$ after some preliminary investigations.

The convergence criterion employed for reaching the steady-state solution is of the form $|Z_{i,j}^{n+1}-Z_{i,j}^{n}|<\delta$, where the super-

Table 1 Transient average Nusselt/Sherwood numbers for different grid size and time step ($N=2$, Le$=1$, and $\varepsilon=1$)

τ \ $\Delta\tau$ / $m\times n$	0.001 23×49	0.0005 45×97	0.0005 23×49
0.050	2.39625	2.35733	2.40364
0.100	1.86989	1.82859	1.87233
0.150	1.66341	1.62600	1.66463
0.200	1.55519	1.52103	1.55591
0.300	1.44943	1.41850	1.44997
0.400	1.40580	1.37637	1.40597
0.500	1.38772	1.35989	1.38780
0.600	1.38011	1.35351	1.38014
0.700	1.37411	1.35077	1.37667
0.800	1.37394	1.34943	1.37492
0.900	1.37335	1.34870	1.37394
1.000	1.37297	1.34827	1.37335
1.100	1.37272	1.34799	1.37297
1.200	1.37254	1.34782	1.37272
1.300	1.37242	1.34770	1.37254
1.400	1.37232	1.34761	1.37242
1.500	1.37226	1.34755	1.37233
1.600	1.37221	1.34751	1.37226
1.700	1.37218	1.34748	1.37221
1.800	1.37215	1.34746	1.37218
1.900	1.37213	1.34744	1.37215
2.000	1.37211	1.34742	1.37213
2.100	1.37209	1.34741	1.37211
2.200	1.37208	1.34740	1.37209
2.300	1.37208	1.34740	1.37208
2.400	1.37207	1.34739	1.37208
2.500	1.37207	1.34739	1.37207

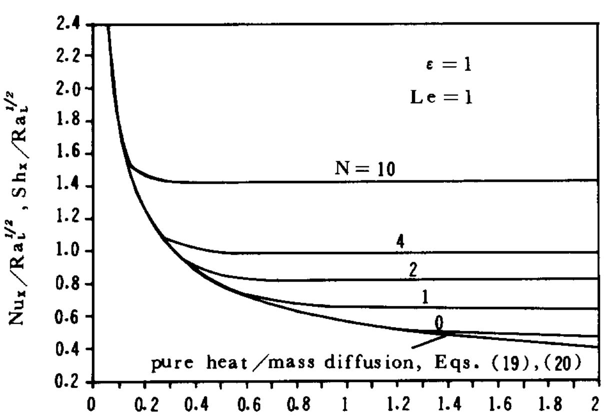

Figure 1 The effect of N on the local Nusselt/Sherwood numbers at $X=1$ for Le$=1$ and $\varepsilon=1$

scripts refer to the number of time steps, the subscripts to the location, and Z represents dependent variables (i.e., velocity, temperature, and concentration). The value of δ is chosen to be 10^{-4}.

Results and discussion

Numerical results are obtained for Le from 0.3 to 100, N from 0 to 10, and for $\varepsilon=0.5$, 1, and 2. Figure 1 shows the effect of N on the pure conduction/diffusion duration time for Le$=1$, $\varepsilon=1$, and $X=1$. It is seen that the time at which the transport changes from the pure conduction/diffusion to convection at a position X decreases with increasing N. This finding can also be verified from the closed-form solution, Equation 25, of the one-dimensional transient. Equation 25 shows that at $X=1$ the time intervals for which the pure conduction/diffusion might be expected to apply locally for $N=10$, 4, 2, 1, and 0 are 0.09, 0.2, 0.333, 0.5, and 1, respectively. These analytical predictions are in good agreement with the finite difference results as seen from Figure 1. Equation 25 indicates that the pure conduction/diffusion time period is independent of Le. The finite difference solutions confirm this prediction, as shown in Figure 2.

Figures 3(a)–(c) show, respectively, the representative transient velocity, temperature, and concentration profiles for Le$=5$, $N=0$, $N=2$, and $\varepsilon=1$ at $X=1$. The similarity solutions for the steady-state flow obtained by Bejan and Khair[1] are also included for comparison. It is seen that the finite-difference solution results for the steady state are in excellent agreement with the similarity solutions.[1] It is observed, from Figures 3(b), (c), that for very small times the temperature and concentration profiles for $N=2$ are identical to those for $N=0$ at each time step for a specified Lewis number. This is due to the fact that,

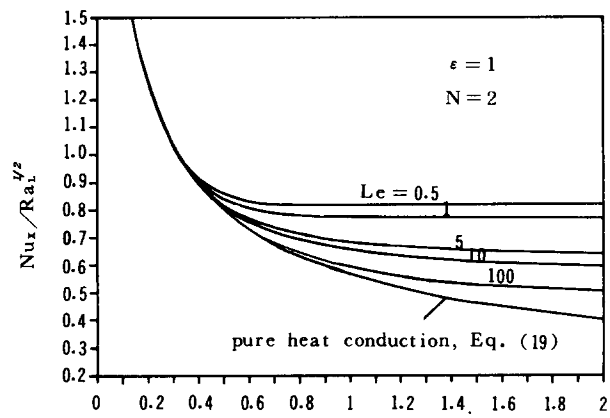

Figure 2 The effect of Le on the local Nusselt numbers at $X=1$ for $N=2$ and $\varepsilon=1$

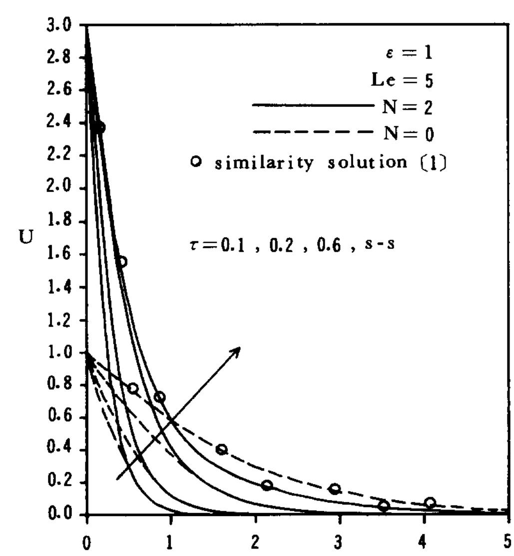

Figure 3(a) The time variation of the transient velocity profiles at $X=1$ for different values of N; Le$=5$, $\varepsilon=1$

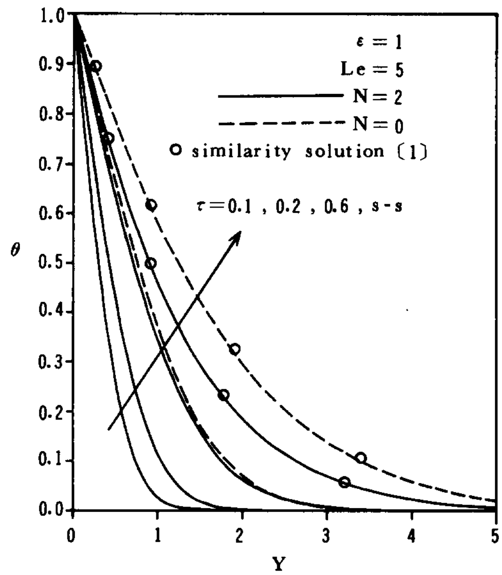

Figure 3(b) The time variation of the transient temperature profiles at $X=1$ for different values of N; Le $=5$, $\varepsilon=1$

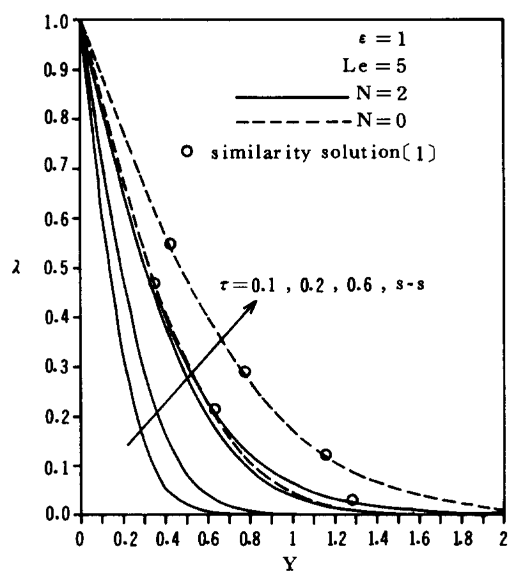

Figure 3(c) The time variation of the transient concentration profiles at $X=1$ for different values of N; Le $=5$, $\varepsilon=1$

at the initial transient, the flowfield is dominated by the one-dimensional heat/mass transport, so convection effects are negligible.

The parameter N does not appear in Equations 19 and 20; therefore the one-dimensional heat/mass transport period is independent of N. However, N plays a prominent role during the full transient period in velocity, as shown in Figure 3(a).

Figures 4(a), (b) show the transient average Nusselt and Sherwood numbers under different values of N for $\varepsilon=1$ and for Le $=0.5$, 5, respectively. It is seen that, for a given Le, a larger N gives rise to higher transient average Nusselt and Sherwood numbers. For a given N and $\varepsilon=1$, the transient Nusselt number is larger than the Sherwood number for Le <1, smaller for Le >1, and identical for Le $=1$.

The influence of Le number on the transient average Nusselt and Sherwood numbers for $N=2$ and $\varepsilon=1$ is exhibited in Figures 5 and 6, respectively. An inspection of these figures reveals that, for a specified N, the Nusselt number decreases as Le increases but Sh increases as Le increases. That is due to the fact that a larger Lewis number is associated with a thicker thermal boundary layer and a thinner concentration boundary layer, and the thicker the thermal/concentration boundary layer, the smaller the surface heat/mass transfer rates.

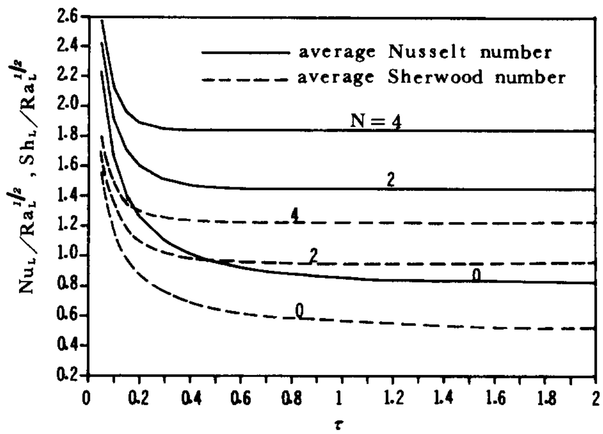

Figure 4(a) The effect of N on the transient average Nusselt and Sherwood numbers for Le $=0.5$ and $\varepsilon=1$

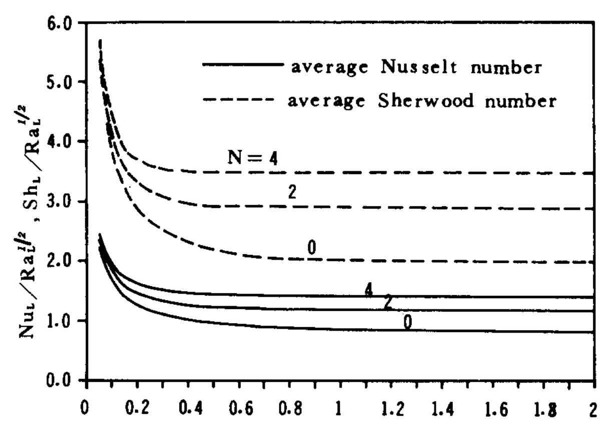

Figure 4(b) The effect of N on the transient average Nusselt and Sherwood numbers for Le $=5$ and $\varepsilon=1$

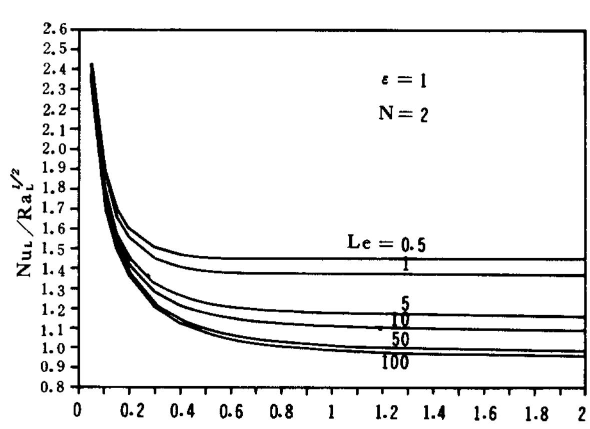

Figure 5 The effect of Le on the transient average Nusselt numbers for $N=2$ and $\varepsilon=1$

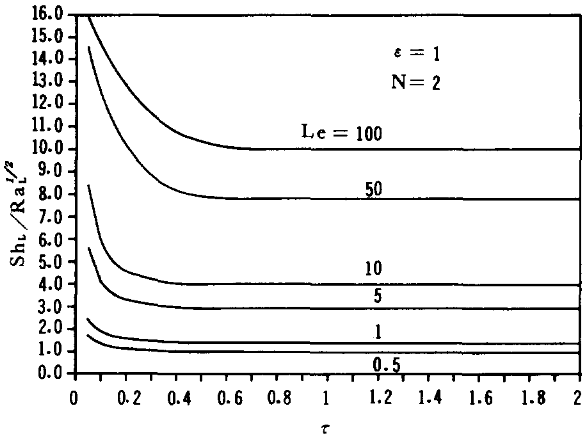

Figure 6 The effect of Le on the transient average Sherwood numbers for $N=2$ and $\varepsilon=1$

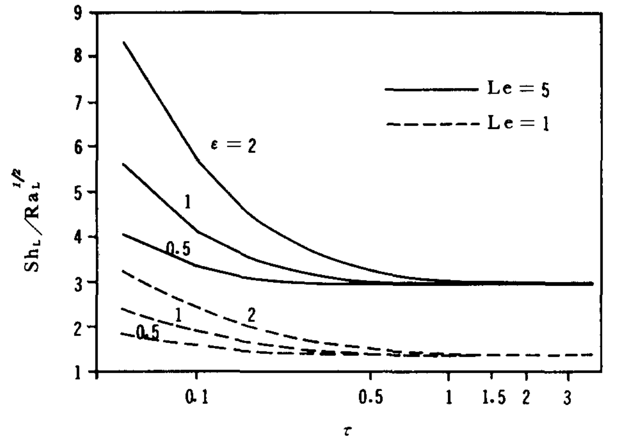

Figure 8 The effect of ε on the transient average Sherwood numbers for $N=2$, Le=1, and Le=5

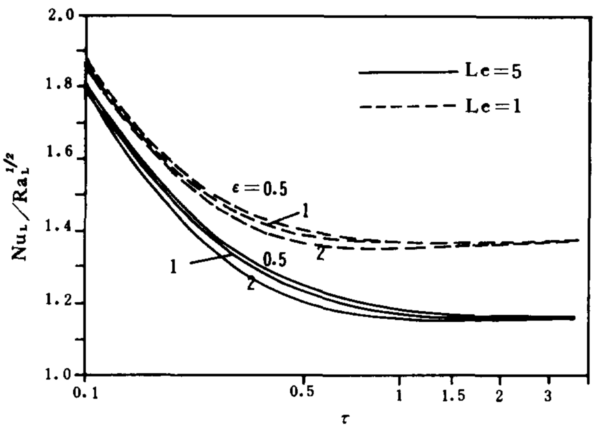

Figure 7 The effect of ε on the transient average Nusselt numbers for $N=2$, Le=1, and Le=5

The time variations of the transient average Nusselt and Sherwood numbers are presented in Figures 7 and 8, respectively, for $\varepsilon=0.5$, 1, and 2. The parameter ε plays a pronounced role during the entire transient period, and its influence diminishes only when the steady-state condition is reached. It is also observed from the figures that the time required to reach the steady state increases as ε increases.

The time required to reach steady-state conditions for various values of N and Le and for $\varepsilon=1$ is summarized in Table 2. For a given Le, it decreases with increasing N. And for a given N, an increase of Le results in a longer transient duration time as $\mathrm{Le}\geq 1$, but in a shorter one as $\mathrm{Le}<1$.

Conclusions

A numerical study has been conducted to analyze the transient laminar natural convection, resulting from the combined effects of heat and mass transfer, along a vertical flat plate embedded in a porous medium subjected to a step change in surface temperature and concentration. The finite-difference results indicate that, for a given Le and ε, the time required to reach the steady state decreases as N increases; for a given N and ε, when $\mathrm{Le}<1$, the time decreases as Le increases, while for $\mathrm{Le}\geq 1$, the reverse trend is true; and for given N and Le, the time increases with an increase of ε. The final steady-state profiles are in good agreement with the similarity solutions.[1]

Table 2 The dimensionless time required to reach steady-state conditions for various N and Le and $\varepsilon=1$

Le \ N	0	1	2	4	10
0.3	3.243	3.156	2.712	2.198	1.483
0.5	3.243	2.690	2.289	1.800	1.217
1.	3.243	2.434	2.053	1.652	1.163
5.	3.243	2.766	2.445	2.008	1.376
10.	3.243	2.995	2.815	2.534	1.966
50.	3.243	3.152	3.088	2.995	2.805
100.	3.243	3.182	3.139	3.076	2.951

A simple relation, $X_{p,\max}=(1+N)\tau$, is obtained for the propagation of the leading-edge effect. The finite-difference solutions during the initial transient are in good agreement with the theoretical prediction. Before this transition occurs, heat transfer is by conduction only and mass transfer is by diffusion only.

References

1. Bejan, A. and Khair, K. R. Heat and mass transfer by natural convection in a porous medium. *Int. J. Heat Mass Transfer*, 1985, **28**, 909–918
2. Trevisan, O. V. and Bejan, A. Natural convection with combined heat and mass transfer buoyancy effects in a porous medium. *Int. J. Heat Mass Transfer*, 1985, **28**, 1597–1611
3. Johnson, C. H. and Cheng, P. Possible similarity solutions for free convection boundary layers adjacent to flat plates in porous media. *Int. J. Heat Mass Transfer*, 1978, **21**, 709–718
4. Ingham, D. B., Merkin, J. H., and Pop, I. Flow past a suddenly cooled vertical flat surface in a saturated porous medium. *Int. J. Heat Mass Transfer*, 1982, **25**, 1916–1919
5. Cheng, P. and Pop, I. Transient free convection about a vertical flat plate embedded in a porous medium. *Int. J. Engng. Sci.*, 1984, **22**, 253–264
6. Ingham, D. B. and Brown, S. N. Flow past a suddenly heated vertical plate in a porous medium. *Proc. R. Soc. Lond.*, 1986, **A403**, 51–80
7. Callahan, G. D. and Marner, W. J. Transient free convection with mass transfer on an isothermal vertical flat plate. *Int. J. Heat Mass Transfer*, 1976, **19**, 165–174
8. Goldstein, R. J. and Briggs, D. G. Transient free convection about vertical plates and cylinders. *J. Heat Transfer, Trans. ASME*, 1964, **86C**, 490–500

9 Gebhart, B. and Dring, R. P. The leading edge effect in transient natural convection flow from a vertical plate. *J. Heat Transfer, Trans. ASME*, 1967, **89C**, 274–275
10 Mahajan, R. L. and Gebhart, B. Leading edge effects in transient natural convection flow adjacent to a vertical surface. *J. Heat Transfer*, 1978, **100**, 731–733
11 Sammakia, B. and Gebhart, B. Transient and steady-state numerical solutions in natural convection. *Numer. Heat Transfer*, 1978, **1**, 529–542
12 Sammakia, B. and Gebhart, B. Transient mixed convection adjacent to a vertical flat plate surface. *Int. J. Heat Mass Transfer*, 1982, **6**, 835–845
13 Rahman, M. M. and Carey, V. P. Steady and transient mixed convection near a vertical uniform heated surface exposed to horizontal fluid flow. *Numer. Heat Transfer*, 1986, **10**, 327–347
14 Carnahan, B., Luther, H. A., and Wilkes, J. O. *Applied Numerical Methods*, Wiley, New York, 1974
15 Anderson, D. A., Tannehill, J. C., and Pletcher, R. H. *Computational Fluid Mechanics and Heat Transfer*, McGraw-Hill, New York, 1984